LBL-27917 Rev.
UC-401
Preprint

Lawrence Berkeley Laboratory
UNIVERSITY OF CALIFORNIA

CHEMICAL SCIENCES DIVISION

Submitted to Journal of Chemical Physics

Crossed Molecular Beam Study of the Reaction $O(^3P)$ + Allene

A.M. Schmoltner, S.Y. Huang, R.J. Brudzynski, P.M. Chu, and Y.T. Lee

May 1992

Prepared for the U.S. Department of Energy under Contract Number DE-AC03-76SF00098

DISCLAIMER

LBL-27917 REV

CROSSED MOLECULAR BEAM STUDY OF THE REACTION O(^{3}P) + ALLENE

A. M. Schmoltner, S. Y. Huang, R. J. Brudzynski
P. M. Chu, and Y. T. Lee

Department of Chemistry
University of California

and

Chemical Sciences Division
Lawrence Berkeley Laboratory
Berkeley, CA 94720 USA

May 1992

This work was supported by the Director, Office of Energy Research, Office of Basic Energy Sciences, Chemical Sciences Division, of the U.S. Department of Energy under Contract No. DE-AC03-76SF00098.

CROSSED MOLECULAR BEAM STUDY OF THE REACTION O(^{3}P) + ALLENE

A. M. Schmoltner, S. Y. Huang, R. J. Brudzynski,
P. M. Chu, and Y. T. Lee

Department of Chemistry
University of California
and
Chemical Sciences Division,
Lawrence Berkeley Laboratory
Berkeley, California 94720, USA

ABSTRACT

The reaction between ground state (^{3}P) oxygen atoms and allene was studied under single collision conditions using the crossed molecular beam method. Product angular distributions and time-of-flight spectra were measured and for each channel the translational energy distribution was determined. Two major reaction channels could be identified unambiguously: the formation of carbon monoxide and ethylene following oxygen atom attack on the central carbon atom, and the formation of hydrogen atom and allenyloxy (formyl-vinyl) radical following oxygen atom attack on the terminal carbon atom. In addition, at least one other reaction channel occurs, tentatively identified as the production of vinyl and formyl radicals. This channel involves the decomposition of acrolein which is formed by the addition of oxygen to the terminal carbon atom, followed by 1,2-hydrogen migration.

Introduction

The reactions of ground state (^3P) oxygen atoms with a variety of simple hydrocarbons have been studied in this laboratory.[1-4] These reactions are of particular importance in combustion chemistry, since they are often responsible for the consumption of the fuel molecules in flames. Here we present our recent investigation of the reaction of $O(^3P)$ with allene.

Two isomers of C_3H_4, allene and methylacetylene, have been identified as intermediates in the combustion of acetylene[5] and aromatic hydrocarbons.[6] The reaction of allene with oxygen atoms has been studied extensively[7-12] and the rate coefficient of this reaction has been determined.[11,13] However, questions remain regarding the mechanism of the reaction and the identity of the primary products.

The accepted general mechanism for reactions of $O(^3P)$ with unsaturated hydrocarbons[14] involves electrophilic addition to the double or triple bond as the first step. In the case of allene, the oxygen atom is thought to add to the central carbon atom[10] forming a triplet diradical, the oxyallyl radical (**1**), which subsequently undergoes ring closure and intersystem crossing (ISC) to form singlet cyclopropanone (**2**). The highly excited cyclopropanone molecule then decomposes into carbon monoxide and ethylene:

$$O(^3P) + C_3H_4 \rightarrow C_2H_4 + CO \qquad (1a)$$

The results of several previous investigations[9-11] indicate that (1a) constitutes the predominant reaction channel.

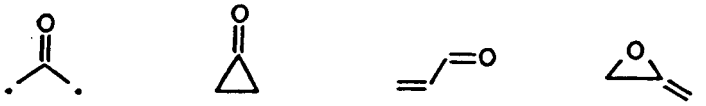

1 2 3 4

However, this does not appear to be the exclusive path in the $O(^3P)$ + allene reaction. Acrolein (3) was identified as a minor product in the gas phase[10] and this species as well as its isomers cyclopropanone (2) and allene oxide (4) were recently detected in a cryogenic matrix as products of the $O(^3P)$ + allene reaction.[7] A channel producing hydrogen atoms and C_3H_3O (1b) was studied by Aleksandrov et al.[12] in a flow tube experiment using resonance fluorescence detection:

$$O(^3P) + C_3H_4 \rightarrow C_3H_3O + H \qquad (1b)$$

The complete mechanism of the $O(^3P)$ + allene reaction is expected to be very complex. Attack of the oxygen atom to either the central or the terminal carbon atom has to be considered. Products can be formed on the initially accessed triplet potential energy surface, or ISC to a singlet state can lead to different sets of products. ISC is required for the formation of the stabilized (singlet) addition products cyclopropanone, allene oxide, or acrolein, and is expected to be facilitated in solid

matrices or at high pressures. However, ISC in an isolated vibrationally excited C_3H_4O reaction intermediate is also likely to be fast, since this was found to be the case in the even smaller C_2H_4O diradical, the intermediate in the reaction of $O(^3P)$ with ethylene.[4]

In analogy to the formation of vinoxy radical and hydrogen atoms in the $O(^3P)$ + ethylene reaction, channel (2a):

$$O(^3P) + C_2H_4 \rightarrow H + CH_2CHO \qquad (2a)$$

hydrogen elimination from the triplet C_3H_4O diradical in the $O(^3P)$ + allene reaction (channel 1b) is expected to occur. Our experiments indeed confirm this assumption, as discussed below.

We also searched for additional product channels. As a possible alternative route on the triplet surface, channel (1c), the formation of ketene and triplet methylene following attack of the central carbon atom was considered:

$$O(^3P) + C_3H_4 \rightarrow CH_2CO + {}^3CH_2 \qquad (1c)$$

Ketene was found in the matrix studies.[7] In our experiments, the detection of the methylene radical or the ketene parent proved to be extremely difficult due to the predominance of nonreactive (elastic and inelastic) signal at m/e=14 and 42. No final conclusions could be drawn on that channel.

Addition of oxygen to the terminal carbon atom leads to the diradical (**5**).

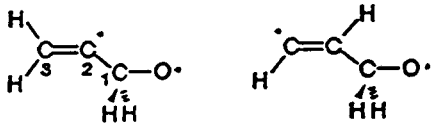

5 6

C_1-C_2 bond rupture in (**5**) would lead to the formation of vinylidene and formaldehyde, channel (1d):

$$O(^3P) + C_3H_4 \rightarrow CH_2C: + CH_2O \qquad (1d)$$

Subsequently, vinylidene can easily rearrange to acetylene.[15]

If ISC is fast and hydrogen atom migration is facile on the singlet surface, as was found to be the case in the $O(^3P)$ + ethylene reaction,[4] additional channels are possible. Hydrogen migration from C_3 in (**5**) to form (**6**) followed by C_1-C_2 bond rupture can lead to the formation of acetylene and formaldehyde, channel (1e):

$$O(^3P) + C_3H_4 \rightarrow C_2H_2 + CH_2O \qquad (1e)$$

The fact that formaldehyde was found in the matrix studies[7] suggests processes (1d) or (1e) as minor channels.

ISC and hydrogen migration in (5) to acrolein (3) followed by C_1-C_2-bond rupture could result in vinyl radical and formyl radical, channel (1f):

$$O(^3P) + C_3H_4 \rightarrow C_2H_3 + CHO \qquad (1f)$$

Table 1 summarizes energetically possible reaction channels considered for the $O(^3P)$ + allene reaction.

Numerous theoretical investigations at both the semi-empirical and ab initio levels have been performed on various parts of the singlet and triplet C_3H_4O-surfaces. The focus of much of the work, especially the earlier studies, was on the relative energies of the isomers cyclopropanone, allene oxide, and oxyallyl radical, and on the question of the stability of cyclopropanone.[24,25,27-35] In addition, the mechanisms of the thermal and photochemical decomposition of cyclopropanone and of the isomerization of cyclopropanone to allene oxide were investigated.[36-39] Recent ab initio calculations,[40] stimulated by our experimental work, focused on the energetics and geometries of the two different modes of oxygen atom approach to allene on the triplet surface and the decomposition routes (1a) and (1b). Chiu and Abidi[41] specifically addressed the question of ISC from triplet oxyallyl to singlet cyclopropanone.

The goal of our work has been to explore the reaction of $O(^3P)$ with allene in the gas phase under single collision conditions. Of particular interest in this system is the question of competition

between decomposition on the triplet surface and triplet→singlet ISC under collision free conditions. The results indicate that similarities with the model system $O(^3P)$ + ethylene exist, but also that interesting additional processes take place.

Experimental

The experimental setup has been described in detail recently.[3] Briefly, a universal crossed molecular beam apparatus[42] was used, where two continuous supersonic molecular beams were crossed at 90° in a high vacuum chamber. The detector consisted of a differentially pumped mass spectrometer equipped with an electron-impact ionizer, quadrupole mass filter, and Daly scintillation ion counter and was rotatable in the collision chamber around the intersection region of the two molecular beams.

The high pressure supersonic oxygen atom beam source employed in these experiments was described by Sibener et al.[43] We used mixtures of 5% O_2 in Ne for all experiments. Only ground state (^3P) oxygen atoms were formed under our experimental conditions.[3] The gas mixture, at pressures from 400 to 600 Torr, was expanded through a quartz nozzle whose diameter varied between 0.10 and 0.25 mm. The dissociation of O_2 was induced by a radio frequency discharge.

The supersonic allene beam was formed by expanding a mixture of 5% allene in helium at a backing pressure of 200-350 Torr through a nozzle of 0.15 mm diameter which was held at room

temperature (for the TOF experiments) or heated to about 80°C (for the angular distribution measurements).

The peak velocities of the oxygen atom beam were between 1.8 and 2.1×10^5 cm/s with speed ratios around 5 and the peak velocity of the allene beam was 1.45×10^5 cm/s with a speed ratio of about 11, resulting in most probable collision energies of 7-8 kcal/mole.

The measurement of the reaction products was carried out in two different ways: First, angular distributions of several masses were measured by modulating one of the beams for background subtraction. Typically, 12 angular scans were obtained for each m/e value, with total counting times of 20 min per angle. Second, TOF distributions were recorded at several laboratory angles and for several masses using the cross-correlation technique.[44] Total accumulation times for the TOF measurements ranged from a few minutes to about two hours depending on the angle and the m/e monitored.

The allene was obtained from Matheson with a stated purity of 95% min. GC/MS analysis was performed on the allene and no impurities were found in detectable amounts. Oxygen/neon mixtures were purchased from Matheson and Airco and had a stated minimum purity of 99.99% and 99.995%, respectively. $^{18}O_2$ with a stated isotopic purity of 95% minimum was kindly provided by Los Alamos National Laboratory and was mixed with neon of 99.995% stated minimum purity purchased from Airco. All gases were used without further purification.

Results and Analysis

Angular distributions for the reaction $O(^3P)$ + allene were measured at various masses, however, meaningful product angular distributions could be obtained only at m/e=53 (C_3HO^+) and 54 ($C_3H_2O^+$). At these masses, only one channel contributes to the signal: the formation of C_3H_3O, reaction (1b). At many other masses of interest, such as m/e=42 (parent mass of ketene) or m/e=14 (parent mass of methylene and major fragment of ketene), fragment ions produced in the dissociative ionization of nonreactively scattered reactants predominate. In the case of m/e=28 (parent mass of both CO and ethylene, major fragment of many species), a large inherent detector background interferes with the measurements.

The angular distribution of m/e=53 is shown in Fig. 1. The direction of the oxygen atom beam corresponds to a laboratory angle of 0°. The error bars represent 95% confidence intervals. The maximum count rates were approximately 8 counts/s. The angular distribution of m/e=54 was found to be superimposable on the m/e=53 distribution after appropriate scaling, but the count rate at this mass was considerably lower. A distinct peak was found whose maximum occurs at an angle close to the direction of the center-of-mass (CM) of the system. Thus the C_3H_3O radical product, recoiling from a light H atom, has a comparatively small CM velocity, and is confined to a small angular range in the laboratory frame, as can be seen in Fig. 1.

When a pair of products with similar or identical masses is produced, such as in the case of the formation of CO and C_2H_4 (channel 1a), both products have the same and relatively large velocities in the CM coordinate system and are therefore scattered over a very large laboratory angular range even at translational energies of only a few kcal/mole. The scanning range of the detector can only probe part of such distributions. We therefore focused our efforts on the measurement of TOF spectra around the direction of the velocity vector of the center-of-mass. They provide a significant amount of dynamic information and allow us to distinguish features due to different reactive and nonreactive channels.

Due to extensive fragmentation in the electron-impact ionizer, signal is often detected at many different ion masses for each product. Parent/daughter-ion relationships can be established by identifying the corresponding features in spectra at different masses. Cross-correlation TOF spectra were obtained at several different angles at the m/e ratios of 14, 25, 26, 27, 28, 29, 30, 31, 32, 40, 41, 42, 52, 53, 54, and 55 using ^{16}O, corresponding to the ions CH_2^+, C_2H^+, $C_2H_2^+$, $C_2H_3^+$, CO^+ or $C_2H_4^+$, CHO^+, CH_2O^+, CH_3O^+, O_2^+, $C_3H_4^+$ or C_2O^+, $^{13}C^{12}C_2H_4^+$ or C_2HO^+, $^{13}C_2{}^{12}CH_4^+$ or $C_2H_2O^+$, C_3O^+, C_3HO^+, $C_3H_2O^+$, and $C_3H_3O^+$, respectively; and at the m/e ratios 30, 31, and 55 using ^{18}O, corresponding to the ions $C^{18}O^+$, $CH^{18}O^+$, and $C_3H^{18}O^+$, respectively.

It should be noted that the TOF spectra at m/e=29 and 30 shown in Figs. 2 and 3 were corrected for an experimental artifact which

was described in detail in our previous paper[3] and has no effect on the results of the data fitting procedure. The signal appearing at flight times of over 300 μs at 50°, 60°, and 70° is also a result of this artifact.

A forward-convolution method was used for the analysis of the reactive scattering data.[45] The goal of the analysis was to find the product translational energy distribution, $P(E_T)$, and the angular distribution in the CM frame, $T(\theta)$. $P(E_T)$ and $T(\theta)$ were assumed to be independent of each other. Furthermore, within the narrow spread of reactant collision energies in our experiment, the relative cross-sections were assumed to be independent of the collision energy. From the $P(E_T)$ and $T(\theta)$ functions, laboratory angular distributions and TOF spectra were calculated and averaged over beam velocities and collision angles as well as the detector acceptance angle and the length of the ionizer and then scaled to the experimental data. This was repeated until a best fit to the experimental data was obtained. For maximum flexibility, the $P(E_T)$ trial functions were not confined to a particular functional form. The $T(\theta)$ functions on the other hand were represented as linear combinations of Legendre polynomials.

<u>C_3H_3O + H channel</u>

M/e=53 was identified as a fragment of C_3H_3O, a product of channel (1b). TOF data for m/e=53 are shown in Fig. 4. The solid lines through the data in Figs. 1 and 4 represent the best fit. The relatively poor fit of the angular distribution at smaller

angles could be due to the nonreactive scattering of impurities coming from the beams.

The translational energy distribution $P(E_T)$, shown in the upper panel of Fig. 5, and the CM angular distribution $T(\theta)$, shown in the upper panel of Fig. 6, fit both the TOF data and the angular distribution simultaneously. The $P(E_T)$ distribution for this channel is very broad, extending to 25 kcal/mole, which corresponds to the total available energy of the system, namely the sum of collision energy, exothermicity (16 kcal/mole[46]), and internal energy left in the allene molecules after the supersonic expansion. Both the energy of maximum probability and the average energy in this distribution are around 12 kcal/mole. The $T(\theta)$ (see Fig. 6) is almost isotropic but shows slight backward peaking with respect to the oxygen beam. The deviation from isotropy for this channel is small and probably insignificant.

The TOF spectra of m/e=52, 53, and 54 showed identical features, m/e=53 having the highest count rates. At m/e=55, the parent mass of C_3H_3O, no peak was found. The data at m/e=55 obtained with ^{18}O were equivalent to the data at m/e=53 using ^{16}O. Furthermore, components due to the fragmentation of $C_3H_3O^+$ could be identified at m/e=29 (CHO^+), m/e=30 ($C^{18}O^+$), and m/e=31 ($CH^{18}O^+$). Fig. 2 shows these components as the slowest features (dashed line, small dashes) at 50°, 60°, and 70° for m/e=29, and Fig. 3 for m/e=30. The fact that no signal was observed at the parent mass of C_3H_3O, m/e=55, is not surprising since in the case of the O + ethylene reaction (2a) the major fragment of vinoxy radical was

found to be at m/e=42, and only very little signal was observed at m/e=43, the parent of vinoxy radical.[2,4]

CO + C_2H_4 channel

Extensive efforts to detect the products of channel (1a), carbon monoxide and ethylene, were initially not successful because of a number of experimental difficulties. The background problems at m/e=28 were overcome by using ^{18}O, enabling us to detect $C^{18}O^+$ at m/e=30.

Fig. 3 shows the m/e=30 TOF spectra at five different laboratory angles. In all five spectra, a sharp and fast feature, which peaks around 55 μs, was identified with $C^{18}O$ from channel (1a). The chain-dashed lines in Fig. 3 represent the best fit for this assumption. The translational energy distribution $P(E_T)$ used is shown in Fig. 7. The CM angular distribution $T(\theta)$ is shown in the lower panel of Fig. 6. The $P(E_T)$ distribution for this channel peaks around 32 kcal/mole and the average translational energy is about 40 kcal/mole. The fit is not very sensitive to the fast end of the distribution due to insufficient resolution for products arriving at the detector in a very short time. It is clear, however, that in this case the distribution does not extend to the total available energy of approximately 126 kcal/mole.

The best fit was obtained using the $T(\theta)$ shown in the lower panel of Fig. 6, which is forward-backward symmetric and slightly forward-backward peaking. The deviations from isotropy are probably not significant in this case, either.

The m/e=30 data at 50°, 60°, and 70° also show slow features (centered around 160 μs) deriving from channel (1b), as mentioned above. Furthermore, all five angles show an additional component with intermediate velocities, indicating the presence of a third channel.

CHO + C_2H_3 channel

The TOF spectra for m/e=30 ($C^{18}O^+$) shown in Fig. 3 clearly show an additional product or products with intermediate velocities which lie in between the fast signal from the CO + C_2H_4 channel (1a) and the slow signal from C_3H_3O + H (1b). The m/e=29 (CHO^+) data also show this component at all angles measured. This signal most likely arises from CHO product.

Since the reaction channel (1b) was found in striking similarity to channel (2a) in the $O(^3P)$ + C_2H_4 reaction, it appears very likely that an analogous reaction to

$$O(^3P) + C_2H_4 \rightarrow CHO + CH_3 \qquad (2b)$$

could occur in the case of allene as well, forming CHO and C_2H_3 as products. This channel would involve a 1,2-hydrogen migration from the carbon atom to which the oxygen atom is bonded and subsequent C_1-C_2 bond rupture. Because 1,2-hydrogen migration on the triplet surface has a high potential energy barrier, at the collision energies of a typical molecular beams experiment this process is only possible if T → S ISC occurs in the initially formed

diradical. In the allene case, the product of this hydrogen migration would be acrolein, and the fragments formyl radical and vinyl radical. Even though neither of these two radicals was identified as a product of the $O(^3P)$ + allene reaction previously, acrolein has been identified in both gas phase and matrix experiments.[7,10]

As can be seen from the fits in Figs. 2 and 3, the production of formyl + vinyl radicals through reaction (1f) can account for the remainder of the reactive scattering signal. The $P(E_T)$ used for this fit (lower panel of Fig. 5) peaks at 5 kcal/mole and has an average translational energy of about 11 kcal/mole and a maximum translational energy of 30 kcal/mole, corresponding to approximately the maximum available energy for this channel. Again, the CM angular distribution $T(\theta)$ could not be determined accurately for (1f). A forward-backward symmetric, strongly forward-backward peaked distribution fit the present data best.

Other possible channels

The identification of the features in the TOF spectra (Figs. 2 and 3) which peak at flight times around 100 μs with CHO from channel (1f) is not unambiguous. Alternatively, we were able to fit this signal using a combination of other channels, such as the formation of ketene and triplet methylene, channel (1c), and the formation of formaldehyde and C_2H_2, channel (1d) or (1e). The possible occurrence of either of these channels can not be excluded based on our data alone, as is a combination of them and channel

(1f). If channel (1f) is indeed contaminated by others to some extent, then the $P(E_T)$ and $T(\theta)$ distributions we are reporting for that channel are uncertain to some degree. It appears unlikely that channel (1e) constitutes a major pathway, since in none of the previous $O(^3P)$ + allene experiments significant amounts of formaldehyde were detected.

Our data also do not rule out the formation of a hydrogen molecule and propadienone:

$$O(^3P) + C_3H_4 \rightarrow CH_2{=}C{=}C{=}O + H_2 \qquad (1h)$$

This channel could contribute to the slow signal in Figs. 2-4 assigned to channel (1b).

Discussion

Table 1 lists several of the energetically accessible reaction channels considered in the $O + C_3H_4$ reaction system, and Figs. 8 and 9 schematically show the triplet and singlet potential energy surfaces involved in the reactions studied. There are large uncertainties in some of the energy levels and particularly in most of the barrier heights.

The initial step in the reaction is electrophilic addition of the oxygen atom to either the central or the terminal carbon atom. The terminal carbon attack channel is expected to resemble that for

$O(^3P)$ addition to C_2H_4. This is confirmed by ab initio MCSCF calculations performed by Lester and coworkers.[40] The entrance channel barrier for the terminal carbon attack was calculated[40a] to be 17.02 kcal/mole which is clearly too high, since reaction was observed at collision energies less than 8 kcal/mole. Similarly, the energy levels calculated by MCSCF for the intermediates and products are expected to be too high. The entrance channel barrier for O + C_2H_4 is known to be very small.[47] However, the value calculated by Dupuis et al.[48,49] using similar methods was also as high as 16 kcal/mole. It can be expected[40] that CI corrections would reduce the calculated values by about 15 kcal/mole.

The resulting diradical (**5**) has a plane of symmetry but is not planar. H elimination from (**5**) leads to allenyloxy (α-formyl-vinyl) radical (**7**).

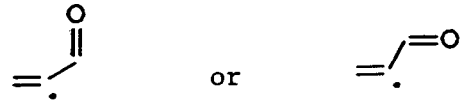

7

The barrier for this process has not been calculated, but is likely to be similar to that for the $CH_2CH_2O \rightarrow CH_2CHO + H$ reaction, or about 18.5 kcal/mole.[18] The C_1-O and C_2-C_3 distances are shorter than the C_1-C_2 distance,[40] indicating a double bond character for the C_1-O and C_2-C_3 bonds in the predicted ground state.

The data we obtained on the ionizer cracking pattern of (**7**) show large ion signals at m/e=29 (CHO^+) and m/e=26 and 27 ($C_2H_2^+$ and

$C_2H_3^+$) similar to the fragmentation of acrolein,[50] indicating a relatively weak C_1-C_2 bond in the parent ion.

The translational energy distribution we obtained is very similar to that for channel (2a) in the ethylene case, but clearly broader. The maximum translational energy corresponds roughly to the available energy calculated assuming the same exothermicity as channel (2a) for $O(^3P)$ + ethylene. The CM angular distribution was found to be isotropic, again very similar to the ethylene case.

For the oxygen atom attacking the central carbon atom of allene, a lower entrance channel barrier than for the terminal carbon attack was calculated by Lester and coworkers, namely 15.16 kcal/mole.[40a] Again, this value must actually lie considerably lower, since reaction (1a) was observed at thermal energies.[9-11]

The oxygen atom approach toward the central carbon atom can be visualized as follows: the two oxygen p-orbitals, each containing one unpaired electron, interact with the two π-orbitals of allene which are orthogonal to each other. The two allene π-bonds are replaced by a C-O σ-bond and a C-O π-bond, respectively, leaving one unpaired electron each on the two outer carbon atoms. The C-C bonds lengthen as the O comes closer, while the C-C-C backbone bends. Assuming no ISC occurs, triplet oxyallyl (**1**) is formed. According to Ref. 40a, the minimum energy path of the reaction leads to a structure where one of the CH_2 groups is rotated 90° with respect to the symmetry plane, corresponding to the H-atom orientation in allene. Its energy was calculated to be 23.5 kcal/mole lower than $O(^3P)$ + allene. The lowest energy structure,

however, was found to be planar (C_{2v} symmetry), with its energy 8.5 kcal/mole below the twisted structure. The barrier, if any, to rotation was not calculated.

Twenty years ago, Hoffmann[35] had already predicted the ground state of oxyallyl to be a triplet. More recently, Osamura et al.[52] calculated the structures of several low lying singlet and triplet states of oxyallyl. The ground state ($^3B_2$) and the first excited state ($^1A_1$) were found to be only 6 kcal/mole apart.

Recent experiments on oxygen-atom transfer from vibrationally excited NO_2 to allene in a cryogenic matrix[51] provided direct information on the nature of the diradical formed in the central carbon attack channel. The fact that the only primary product observed under these conditions was the 2-allyl nitrite radical indicates that the oxyallyl is formed in a state where one unpaired electron resides on the oxygen atom, i.e. the ($^1B_1$) or the ($^3B_1$) state.[52]

Triplet → singlet ISC has to take place in order for cyclopropanone to be formed from triplet reactants. A process where orbital angular momentum and spin are changed simultaneously can provide the mechanism for efficient ISC.[40b,41] Several electronic states of oxyallyl which are close in energy possibly facilitate the conversion. Sevin et al.[37] have determined the approximate position of a crossing point at ≤ 55 kcal/mole above the ground state of cyclopropanone, using ab initio calculations without complete geometry optimization.

The decomposition of cyclopropanone has received much attention. The calculations by Sevin et al.[37] indicate that the lowest energy pathway from ground state cyclopropanone is actually C_2-C_3 bond scission, resulting in the oxyallyl diradical. This is in accord with the experimental results of Rodriguez et al.[23] who found that the thermal reaction produced no volatile substances but only a polymer. C_1-C_2 scission on the other hand requires a higher activation energy (about 80 kcal/mole) and an additional 15 kcal/mole to overcome the barrier to completely dissociate the molecule to form CO and C_2H_4.[37]

The photochemical reaction, on the other hand, following excitation to the $^1n\pi^*$ state, should proceed along the C_1-C_2 scission/CO extrusion channel, since the barrier for this was found[37] to be considerably lower than for C_2-C_3 bond scission. A surface crossing is required to reach the ground states of the products CO and C_2H_4. The results of the ab initio calculations by Yamabe et al.[38] indicate that this process is "bent-in-plane", where the C-C-C-O plane continues to be the plane of symmetry. It is possible that channel (1a) involves the triplet or singlet $n\pi^*$ state of cyclopropanone, rather than the ground state.

Lin et al.[9] measured the distributions of CO vibrational energy in the reactions of $O(^3P)$ with allene and methylacetylene. In the case of the allene reaction, excitation up to v=7 was found for CO, corresponding to a Boltzmann vibrational temperature of 5100±100K or an average vibrational energy of 6.8 kcal/mole. These values were found to be consistent with a statistical model where

the energy in the cyclopropanone is completely randomized, and assuming CO and C_2H_4 are so loosely bound that they could rotate freely. This is in partial agreement with the theoretical result[37,38] that the dissociation is not a one-step process with a tight transition state but proceeds through an open $\bullet CO-CH_2-CH_2\bullet$ diradical. However, ab initio calculations[37,38] also predict a large exit barrier from the diradical. It is a tight transition state rather than a loose one with freely rotating CO and C_2H_4.

The results of our experiments suggest that in channel (1a) a large amount of energy is channelled into translation, indicating a repulsive interaction upon separation of the closed shell products, in agreement with a large exit barrier potential predicted by the ab initio calculations.

While ab initio calculations already provide a great deal of information on channels (1a) and (1b), little theoretical work has been done on any of the other channels mentioned above. In particular, oxygen atom attack on the terminal carbon followed by 1,2-hydrogen migration to acrolein has not been considered. However, the occurrence of channel (1g), formation of acrolein, has been observed in condensed phase[7] and high pressure gas phase[10] experiments. No information is available on the hydrogen migration barrier, but it can be assumed that it would be high on the triplet surface. In analogy to the C_2H_4/O system, ISC is expected to occur followed by facile 1,2-hydrogen migration on the singlet surface. Fueno and co-workers suggest no barrier for 1,2-hydrogen migration in the $^1C_2H_4O$ case.[53]

The singlet/triplet splittings in CH_2CH_2O were found to be less than 3 kcal/mole[49] and about 6 kcal/mole for the two lowest states of oxyallyl,[52] suggesting a similarly small value for CH_2CCH_2O.

Under single collision conditions the highly excited acrolein could not survive for hundreds of microseconds required to reach our detector, but will fragment instead. Rupture of the C_1-C_2 bond, leading to vinyl and formyl radicals, was found to be the major channel in the mercury sensitized decomposition[54] and the UV-photodissociation[55] of acrolein. Shinohara and Nishi[55] reported a translational energy distribution for the 193 nm photodissociation of acrolein which is qualitatively similar to our $P(E_T)$ shown in the lower panel of Fig. 5. Their distribution, obtained by a direct inversion method from the TOF data, peaks at about 10 kcal/mole and extends to 60 kcal/mole. Their experiment was insensitive to low energy products ($\leq$2 kcal/mole) due to geometric constraints. Furthermore, two-photon processes clearly play a role in their experiment. The authors suggest $S_2 \rightarrow S_1$ internal conversion followed by fragmentation as the major dissociation mechanism at 193 nm.

The translational energy distribution obtained for channel (1f) from our data (lower panel of Fig. 5) peaks at about 5 kcal/mole and is very similar to that obtained for channel (2b) in the O + C_2H_4 reaction.[4] The fact that the distribution does not peak at 0 kcal/mole translational energy but instead at a small, but finite value indicates that there is probably a small barrier to the C-C bond rupture process in both cases. It is very likely

that the radical products went undetected in the earlier bulk experiments or reacted further to the final products observed.

Some of the C_3H_3O in our experiment could be formed on the singlet rather than the triplet surface. The broad $P(E_T)$ (upper panel of Fig. 5) suggests possible additional sources of this product, e.g. hydrogen elimination from acrolein (see Fig. 8). Furthermore, the maximum translational energy in the upper panel of Fig. 5 could not be determined exactly due to the limited energy resolution of this experiment. $P(E_T)$ distributions including translational energies beyond 25 kcal/mole could fit the C_3H_3O data as well.

Possible additional channels such as (1c), (1d), (1e) and (1h) have been mentioned above, but neither our nor previous work provided evidence for them to be major channels.

None of the isomers of the C_3H_4O adduct could be detected in our experiments, since under single collision conditions these highly excited molecules have no chance to stabilize but fragment instead.

Summary

The crossed molecular beam experiment conducted under single collision conditions produced detailed information on major reaction channels of the $O(^3P)$ + allene reaction. Previously the major reaction channel was thought to be (1a), the formation of carbon monoxide and ethylene, and evidence for the occurrence of this process was found in our experiments also. In addition, we unambiguously identified channel (1b), formation of hydrogen atom and allenyloxy (formyl-vinyl) radical.

Our data suggest at least one additional major channel, tentatively identified as (1f), formation of vinyl and formyl radicals from fragmentation of vibrationally excited acrolein. Other minor reaction paths are possible, however, they can not be distinguished in our data.

While channels (1b) and (1f) suggest large similarities between the reaction of $O(^3P)$ atoms with allene and with ethylene, channel (1a) is specific to allene. Apparently, in the reaction of $O(^3P)$ with allene there are two site specific attacks by the oxygen atoms. When $O(^3P)$ attacks the central carbon atom, the formation of a cyclopropanone intermediate leads to the production of CO and C_2H_4. When $O(^3P)$ attacks the central carbon atom, the direct hydrogen substitution (channel 1b) competes with intersystem crossing. When the triplet intermediate becomes a singlet, H migration becomes facile and the formation of acrolein precedes the production of formyl and vinyl radicals.

Acknowledgements

We wish to thank Dr. George H. Kwei for kindly providing us with the $^{18}O_2$. We also wish to thank J. Allman and Dr. R. Ferrieri for technical assistance. Some of the equipment used in this experiment was provided by the Office of Naval Research. This work was supported by the Director, Office of Energy Research, Office of Basic Energy Sciences, Materials Sciences Division of the U.S. Department of Energy under Contract No. DE-AC03-76SF00098.

References

1. S. J. Sibener, R. J. Buss, P. Casavecchia, T. Hirooka, and Y. T. Lee, J. Chem. Phys. 72, 4341 (1980); R. J. Baseman, R. J. Buss, P. Casavecchia, and Y. T. Lee, J. Am. Chem. Soc. 106, 4108 (1984).
2. R. J. Buss, R. J. Baseman, G. He, and Y. T. Lee, J. Photochem. 17, 389 (81).
3. A. M. Schmoltner, P. M. Chu, and Y. T. Lee, J. Chem. Phys. 91, 5365 (1989).
4. A. M. Schmoltner, P. M. Chu, R. J. Brudzynski, and Y. T. Lee, J. Chem. Phys. 91, 6926 (1989).
5. K. H. Homann, J. Warnatz, and C. Wellmann, Sixteenth Symposium (International) on Combustion (Combustion Institute, Pittsburgh, 1977), p. 853; K. H. Homann and H. Schweinfurth, Ber. Bunsenges. Phys. Chem. 85, 569 (1981); K. H. Homann and Ch. Wellmann, Ber. Bunsenges. Phys. Chem. 87, 609 (1983).
6. J. D. Bittner and J. B. Howard, Eighteenth Symposium (International) on Combustion (Combustion Institute, Pittsburgh, 1981), p. 1105.
7. K. A. Singmaster and G. C. Pimentel, J. Mol. Structure 194, 215 (1989).
8. K. A. Singmaster and G. C. Pimentel, J. Mol. Structure 200, 225 (1989).
9. M. C. Lin, R. G. Shortridge, and M. E. Umstead, Chem. Phys. Lett. 37, 279 (1976).

10. J. J. Havel, J. Am. Chem. Soc. 96, 530 (1974).

11. P. Herbrechtsmaier and H. G. Wagner, Ber. Bunsenges. Phys. Chem. 76, 517 (1972).

12. E. N. Aleksandrov, V. S. Arutyunov, and S. N. Kozlov, Kinet. Katal. 21, 1327 (1980).

13. R. Atkinson and J. N. Pitts, Jr., J. Chem. Phys. 67, 2492 (1977); W. S. Nip, D. L. Singleton, and R. J. Cvetanovic, Can. J.Chem. 57, 949 (1979).

14. R. Cvetanovic, Adv. Photochem. 1, 115 (1963).

15. A. C. Scheiner and H. F. Schaefer III, J. Am. Chem. Soc. 107, 4451 (1985).

16. M. W. Chase, Jr., C. A. Davies, J. R. Downey, Jr., D. J. Frurip, R. A. McDonald, and A. N. Syverud, J. Phys. Chem. Ref. Data 14 (1985), Supplement No. 1: JANAF Thermochemical Tables, Third Edition.

17. J. B. Pedley, R. D. Naylor, and S. P. Kirby, Thermochemical Data of Organic Compounds (Chapman and Hall, London, 1986).

18. C. F. Melius, to be published.

19. R. L. Nuttal, A. H. Laufer, and M. V. Kilday, J. Chem. Thermodynamics 3, 167 (1973).

20. A. M. Wodtke, E. J. Hintsa, J. Somorjai, and Y. T. Lee, Isr. J. Chem.

21. M.-C. Chuang, M. F. Foltz, and C. B. Moore, J. Chem. Phys. 87, 3855 (1987).

22. Z. B. Alfassi and D. M. Golden, J. Am. Chem. Soc. 95, 319 (1973).

23. H. J. Rodriguez, J.-C. Chang, and T. F. Thomas, J. Am. Chem. Soc. 98, 2027 (1976).

24. A. Liberles, A. Greenberg, and A. Lesk, J. Am. Chem. Soc. 94, 8685 (1972).

25. J. F. Liebman and A. Greenberg, J. Org. Chem. 39, 123 (1974).

26. E. Block, R. E. Penn, M. D. Ennis, T. A. Owens, and S.-L. Yu, J. Am. Chem. Soc. 100, 7436 (1978).

27. O. Kikuchi, H. Nagata, and K. Morihashi, J. Mol. Structure (Theochem) 124, 261 (1985).

28. P. M. Lahti, A. R. Rossi, and J. A. Berson, J. Am. Chem. Soc. 107, 2273 (1985).

29. L. J. Schaad and B. A. Hess, Jr., J. Org. Chem. 46, 1909 (1981).

30. R. C. Bingham, M. J. S. Dewar, and D. H. Lo, J. Am. Chem. Soc. 97, 1302 (1975).

31. M. E. Zandler, C. E. Choc, and C. K. Johnson, J. Am. Chem. Soc. 96, 3317 (1974).

32. A. Liberles, S. Kang, and A. Greenberg, J. Org. Chem. 38, 1922 (1973).

33. J. F. Olsen, S. Kang, and L. Burnelle, J. Mol. Structure 9, 305 (1971).

34. N. Bodor, M. J. S. Dewar, A. Harget, and E. Haselbach, J. Am. Chem. Soc. 92, 3854 (1970).

35. R. Hoffmann, J. Am. Chem. Soc. 90, 1475 (1968).

36. J. V. Ortiz, J. Org. Chem. 48, 4744 (1983).

37. A. Sevin, E. Fazilleau, and P. Chaquin, Tetrahedron 37, 3831 (1981).

38. S. Yamabe, T. Minato, and Y. Osamura, J. Am. Chem. Soc. 101, 4525 (1979).

39. D. M. Hayes, C. A. Zeiss, and R. Hoffmann, J. Phys. Chem. 75, 340 (1971).

40. (a) B. L. Hammond, S. Y. Huang and W. A. Lester, Jr., J. Phys. Chem. 94, 7969 (1990); (b) S. Y. Huang, Ph. D. Thesis, University of California, Berkeley, 1988.

41. Y.-N. Chiu and M. S. F. A. Abidi, J. Phys. Chem. 86, 3288 (1982).

42. Y. T. Lee, J. D. McDonald, P. R. LeBreton, and D. R. Herschbach, Rev. Sci. Instrum. 40, 1402 (1969).

43. S. J. Sibener, R. J. Buss, C. Y. Ng, and Y. T. Lee, Rev. Sci. Instrum. 51, 167 (1980).

44. K. Sköld, Nucl. Instrum. Methods 63, 114 (1968); V. L. Hirschy and J. P. Aldridge, Rev. Sci. Instrum. 42, 381 (1971); G. Comsa, R. David, and B. J. Schumacher, Rev. Sci. Instrum. 52, 789 (1981).

45. R. J. Buss, Ph. D. Thesis, University of California, Berkeley, 1979; A. M. Schmoltner, Ph. D. Thesis, University of California, Berkeley, 1989.

46. Assumed to be same as the exothermicity of the $O(^3P) + C_2H_4 \rightarrow H + C_2H_3O$ channel in Ref. 18.

47. Crossed-beams experiments (A. R. Clemo, G. L. Duncan, and R. Grice, Trans. Faraday Soc. 2, 78, 1231 (1982); 79, 637 (1983))

determined a threshold of 1.2±0.7 kcal/mole; the bulk activation energy was found to be 1.5-1.6 kcal/mole, assuming that the first term in the biexponential expression corresponds to the addition reaction (K. Mahmud, P. Marshall, and A. Fontijn, J. Phys. Chem. 91, 1568 (1987); R. B. Klemm, F. L. Nesbitt, E. G. Skolnik, J. H. Lee, and J. F. Smalley, J. Phys. Chem. 91, 1574 (1987)); and recent BAC-MP4 calculations (Ref. 18) yielded a value of 0.6 kcal/mole.

48. M. Dupuis, J. J. Wendoloski, T. Takada, and W. A. Lester, Jr., J. Chem. Phys. 76, 481 (1982).

49. M. Dupuis, J. J. Wendoloski, and W. A. Lester, Jr., J. Chem. Phys. 76, 488 (1982).

50. Atlas of Mass Spectral Data, E. Stenhagen, S. Abrahamsson, and F. W. McLafferty, editors, Vol. 1 (Wiley, New York, 1969).

51. M. Nakata and H. Frei, J. Am. Chem. Soc. 114, in press; H. Frei, in Vibrational Spectra and Structure, Vol. 21, J. R. Durig, editor (Elsevier, Amsterdam, 1992).

52. Y. Osamura, W. T. Borden, and K. Morokuma, J. Am. Chem. Soc. 106, 5112 (1984).

53. Y. Takahara, K. Yamaguchi, and T. Fueno, Book of Abstracts, Third Symposium on Chemical Reactions, Tokyo University, June 3-5, 1987.

54. A. G. Harrison and F. P. Lossing, Can. J. Chem. 37, 1696 (1959).

55. H. Shinohara and N. Nishi, J. Chem. Phys. 77, 234 (1982).

Table 1. Exothermicities ($\Delta H^{\circ}_{f,298}$) for various $O(^3P)$ + allene reaction channels

Reaction	Exothermicity (kcal/mole)	Sources
(1a) $O + C_3H_4 \rightarrow C_2H_4 + CO$	-119.4	a,b
(1b) $O + C_3H_4 \rightarrow CH_2{=}C\cdot{-}CHO + H$	-18.5	c
(1c) $O + C_3H_4 \rightarrow CH_2CO + {}^3CH_2$	-24.6	a,b,d
(1d) $O + C_3H_4 \rightarrow CH_2{=}C{:} + CH_2O$	-39.5	a,b,e
(1e) $O + C_3H_4 \rightarrow HC{\equiv}CH + CH_2O$	-79.0	a,b
(1f) $O + C_3H_4 \rightarrow C_2H_3 + CHO$	-25	a,b,f,g
(1g) $O + C_3H_4 \rightarrow$ acrolein	-123.2	a,b,h
$O + C_3H_4 \rightarrow$ cyclopropanone	-101.7	a,b,i
$O + C_3H_4 \rightarrow$ allene oxide	-80	j
(1h) $O + C_3H_4 \rightarrow CH_2{=}C{=}C{=}O + H_2$	-82	k
(1i) $O + C_3H_4 \rightarrow CH_2{=}CH{-}\dot{C}O + H$	-36	a,b,i

(a) Ref. 16, (b) Ref. 17, (c) assumed to be the same as for reaction (2a) (Ref. 18), (d) Ref. 19, (e) Ref. 18, (f) Ref. 20, (g) Ref. 21, (h) Ref. 22, (i) Ref. 23, (j) allene oxide is assumed to lie about 22 kcal/mole higher in energy than cyclopropanone, see Refs. 24-27, (k) taken to be the same as for reaction (2c) (Ref. 18).

Figure Captions

Fig. 1 Laboratory angular distribution of the C_3H_3O product at m/e=53 (C_3HO^+). Angles are measured from the oxygen atom beam. Scattered points: measured data points; dashed line: fit.

Fig. 2 Time-of-flight spectra for products at m/e=29 (HCO^+) at four different laboratory angles. Dashed lines (short dashes): fits for components due to channel (1b); dashed lines (long dashes): fits for components due to channel (1f); solid lines: sum of the fits for channels (1b) and (1f). Calculated curves are scaled to the data for each angle and each channel separately.

Fig. 3 Time-of-flight spectra for products at m/e=30 ($C^{18}O^+$) at five different laboratory angles. Dashed lines (short dashes): fits for components due to channel (1b); dashed lines (long dashes): fits for components due to channel (1f); chain-dashed lines: fits for components due to channel (1a); solid lines: sum of the fits for the individual channels. Calculated curves are scaled to the data for each angle and each channel separately.

Fig. 4 Time-of-flight spectra for products at m/e=53 (C_3HO^+) at three different laboratory angles. Solid lines: fits, scaled to the data for each angle separately.

Fig. 5 Translational energy distributions $P(E_T)$ for channels (1b), upper panel, and (1f), lower panel.

Fig. 6 Center-of-mass angular distributions $T(\theta)$ for channels (1b), upper panel, and (1a), lower panel.

Fig. 7 Translational energy distribution $P(E_T)$ for channel (1a).

Fig. 8 Schematic energy diagram for the terminal carbon attack channels in the reaction of $O(^3P)$ with allene. Solid lines: triplet surfaces; dashed lines: singlet surfaces.

Fig. 9 Schematic energy diagram for the central carbon attack channels in the reaction of $O(^3P)$ with allene. Solid lines: triplet surfaces; dashed lines: singlet surfaces.

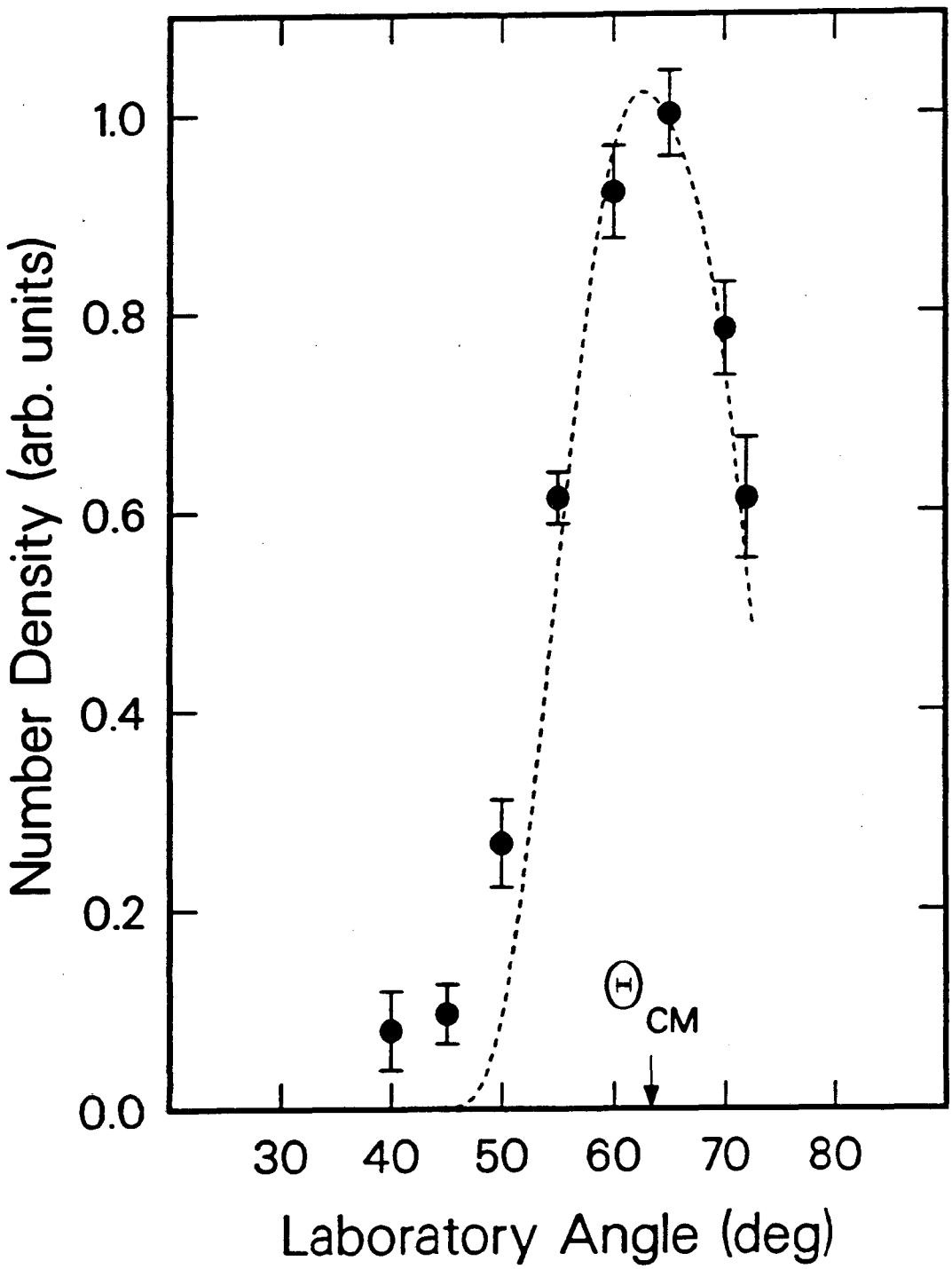

XBL 899-3194

Fig. 1

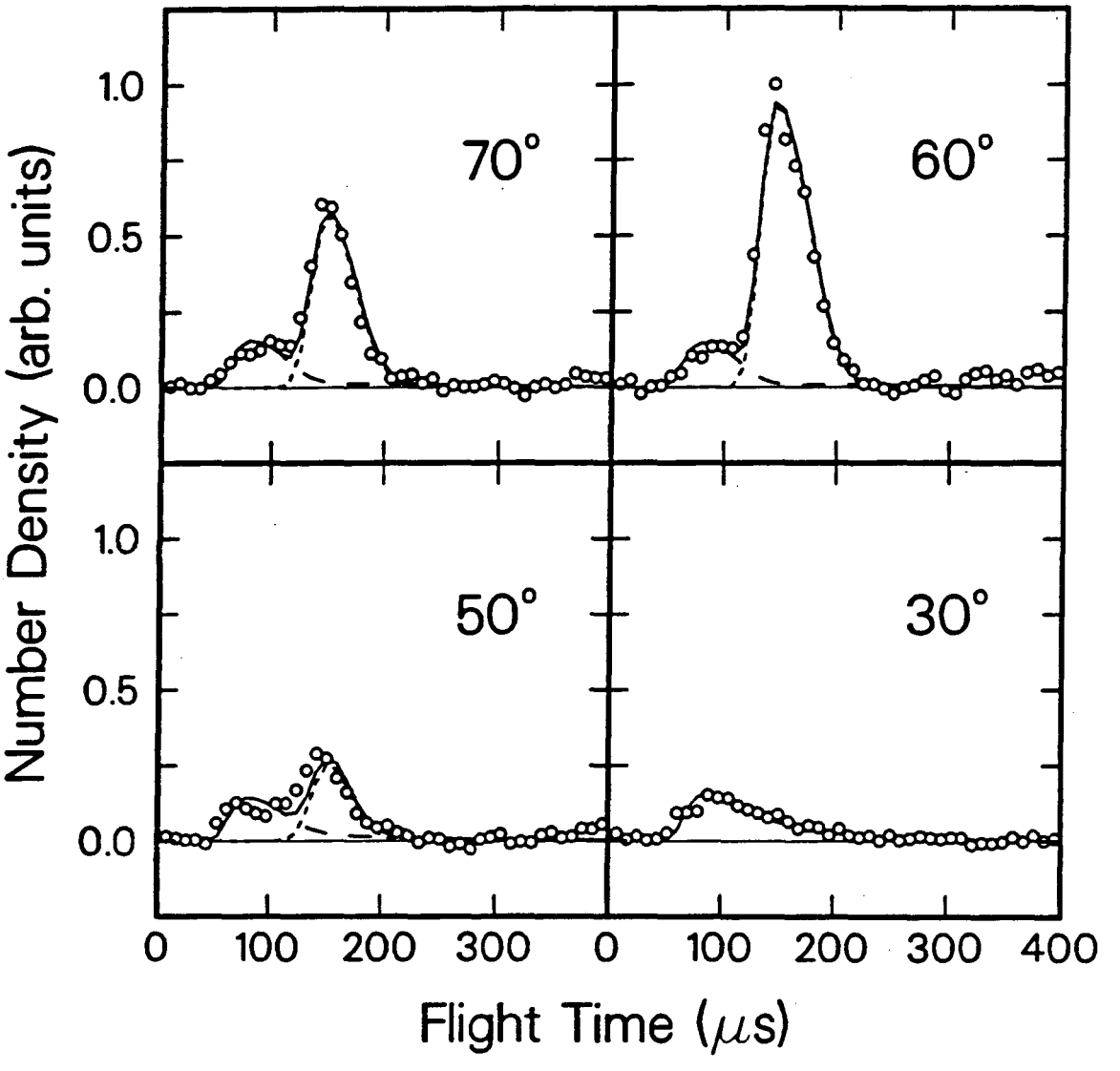

XBL 899-3198

Fig. 2

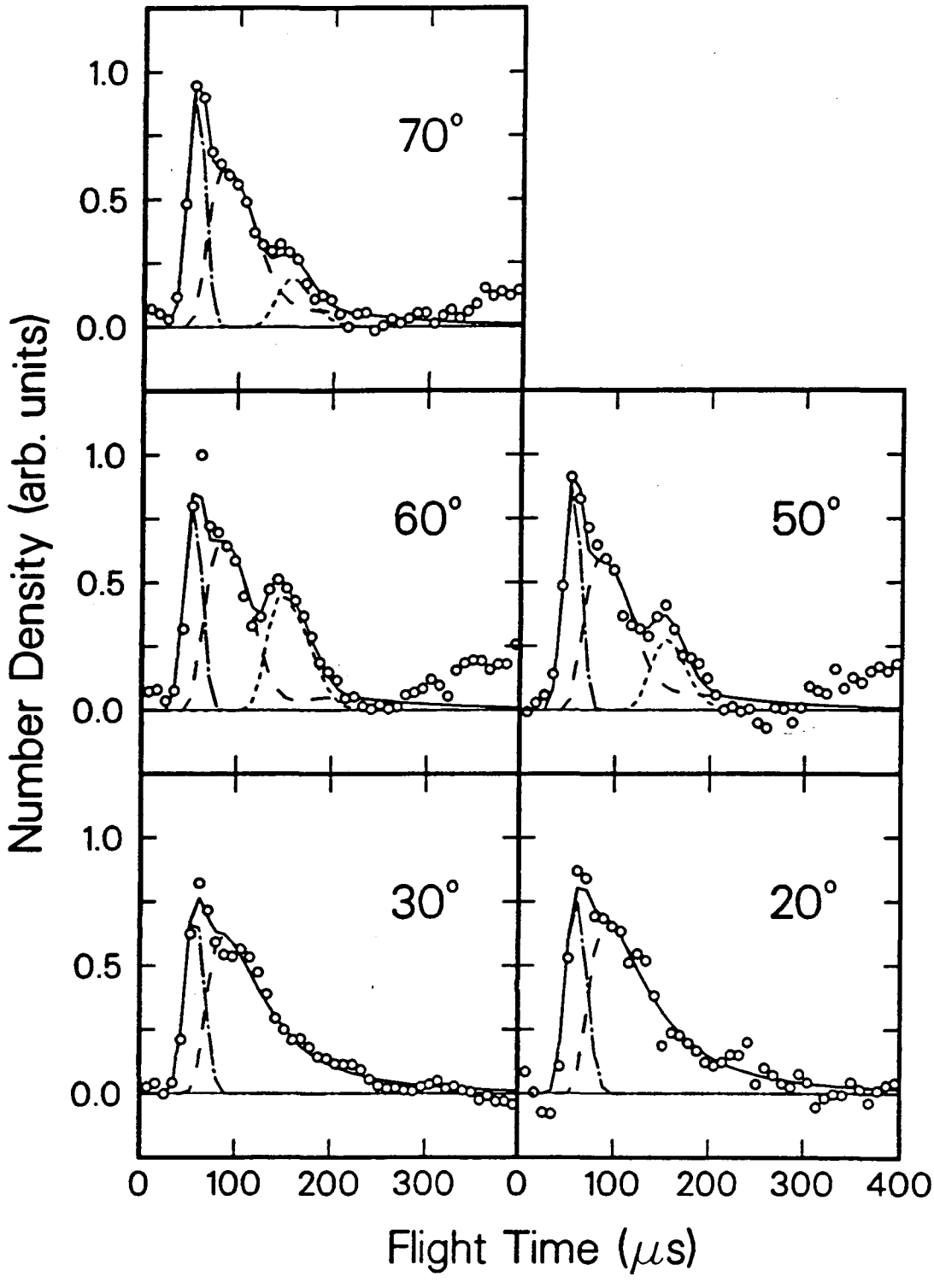

Fig. 3

XBL 899-3200

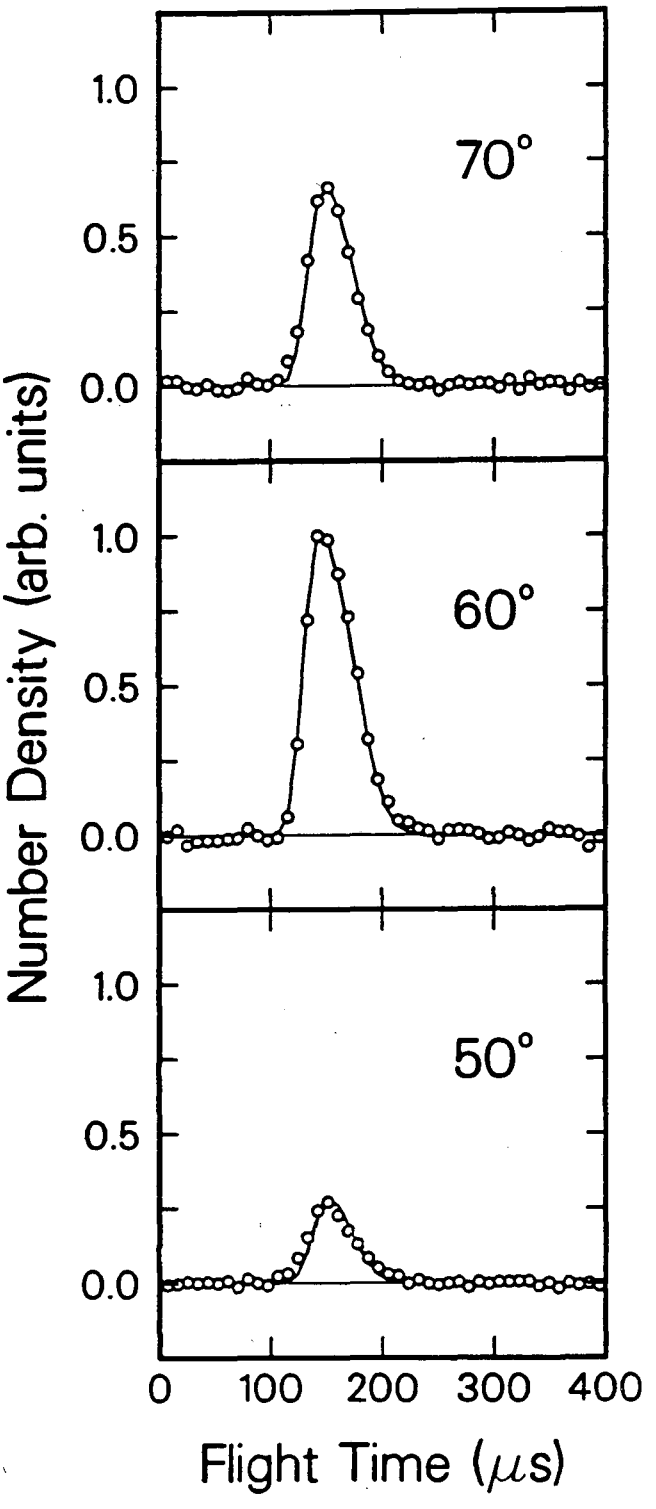

XBL 899-3199

Fig. 4

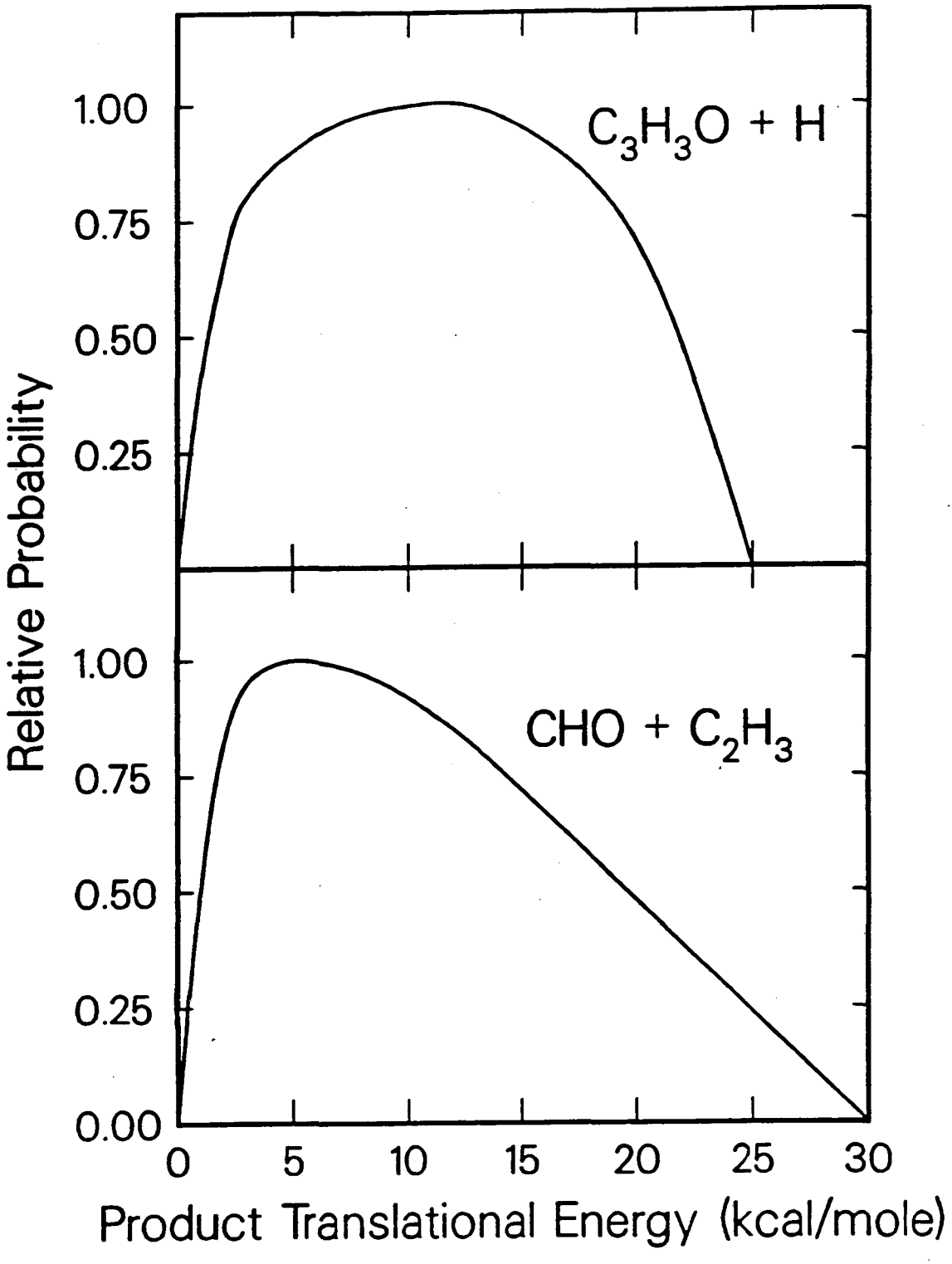

XBL 899-3196

Fig. 5

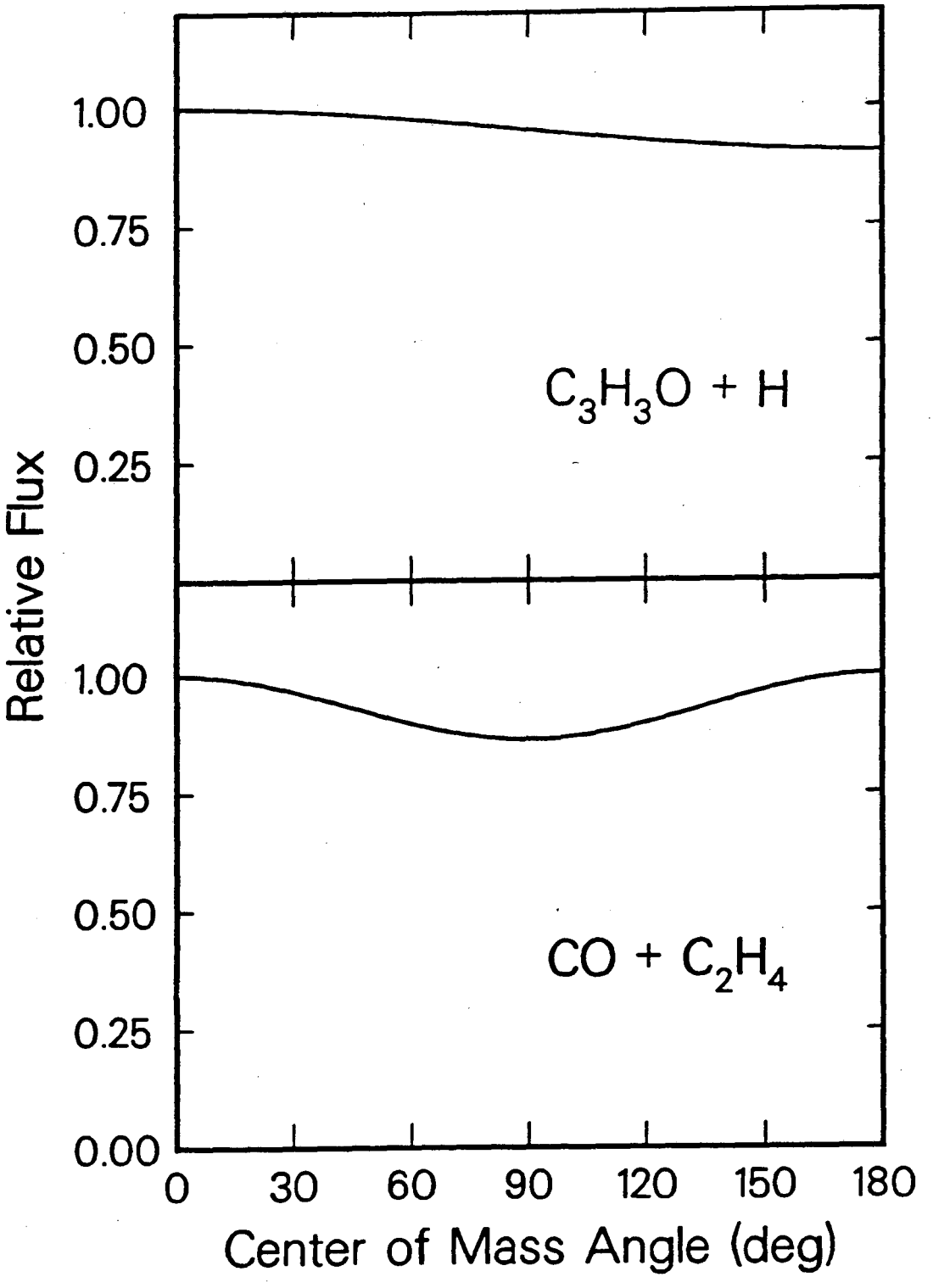

XBL 899-3195

Fig. 6

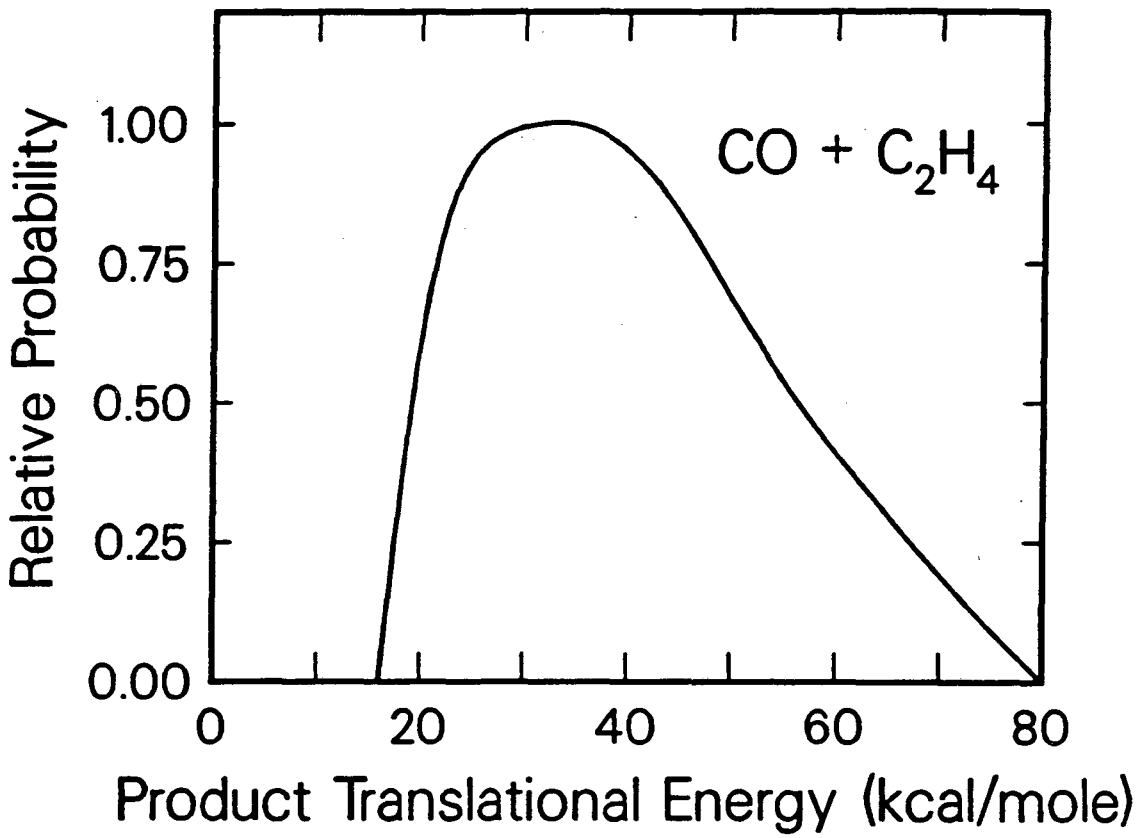

XBL 899-3197

Fig. 7

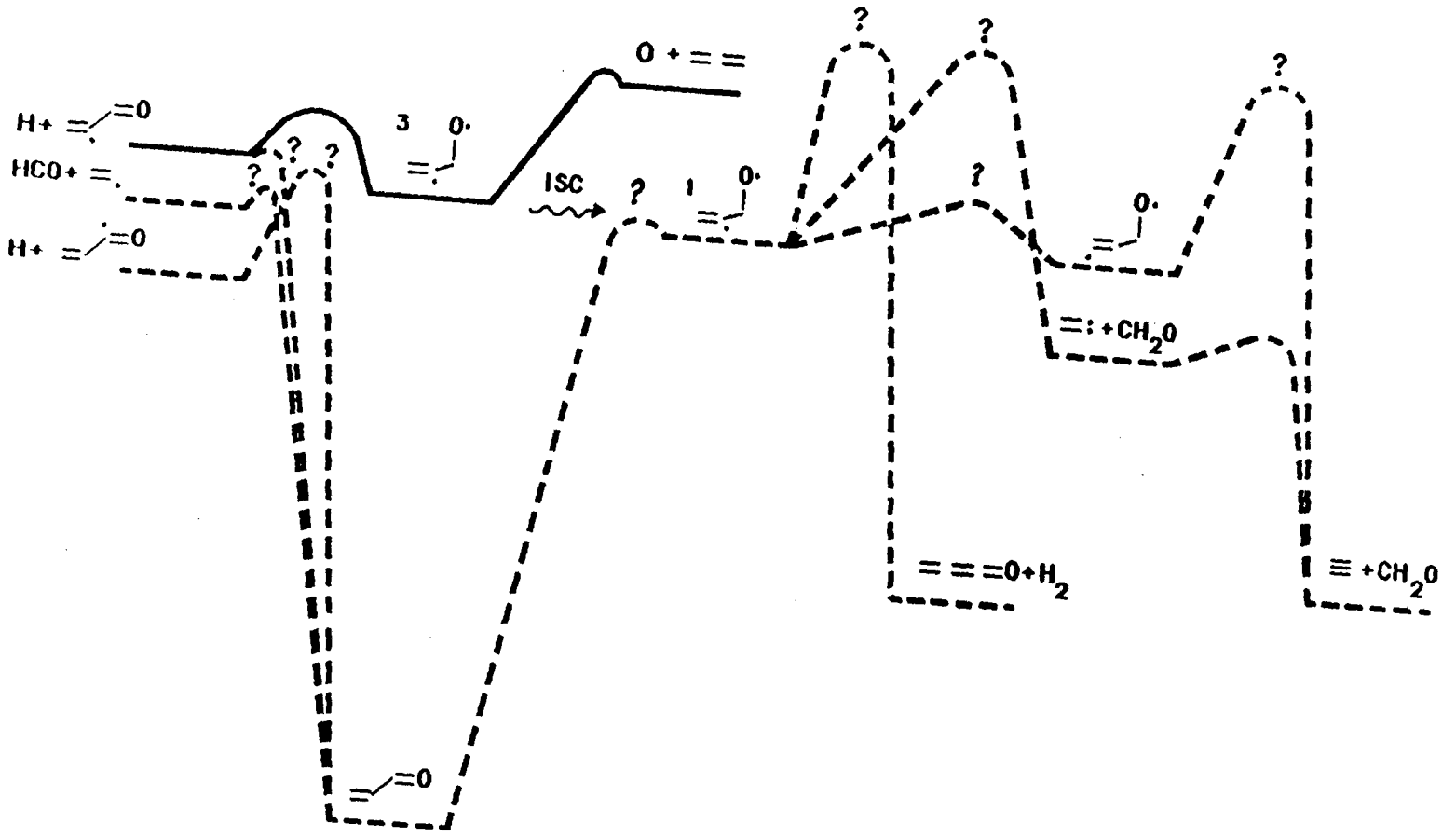

XBL 899-3202

Fig. 8

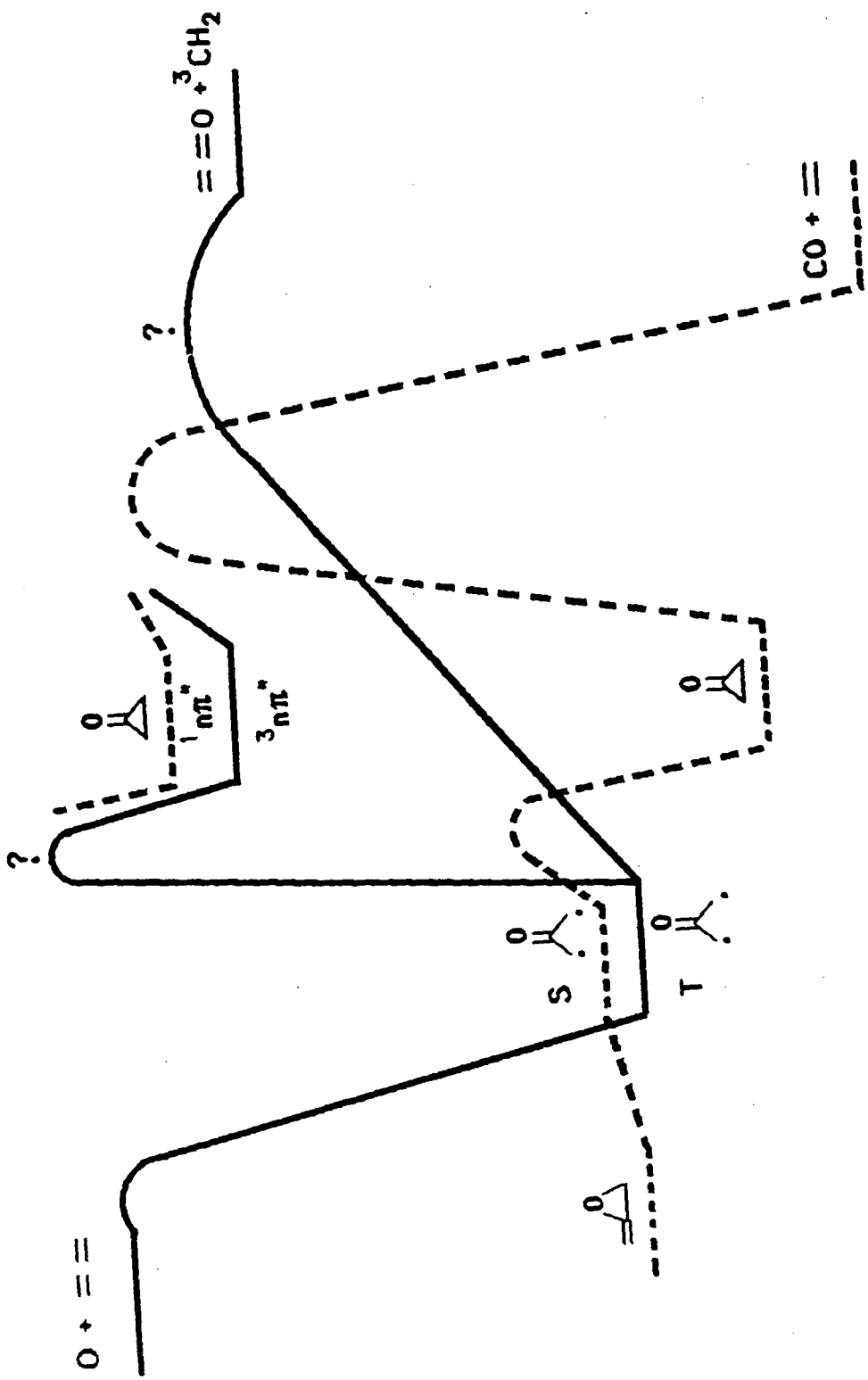

XBL 899-3201

Fig. 9

LAWRENCE BERKELEY LABORATORY
UNIVERSITY OF CALIFORNIA
TECHNICAL INFORMATION DEPARTMENT
BERKELEY, CALIFORNIA 94720